

Improving Downlink Coordinated Multipoint Performance in Heterogeneous Networks

Faris B. Mismar, *Senior Member, IEEE*, and Brian L. Evans, *Fellow, IEEE*

Abstract—We propose a novel method for practical Joint Processing downlink coordinated multipoint (DL CoMP) implementation in LTE/LTE-A systems using supervised machine learning. DL CoMP has not been thoroughly studied in previous work although cluster formation and interference mitigation have been studied extensively. In this paper, we attempt to improve the cell edge data rate served by a heterogeneous network cluster by means of dynamically changing the DL SINR threshold at which the DL CoMP feature is triggered. We do so by using a support vector machine (SVM) classifier. The simulation results show a cell edge user throughput improvement of 33.3% for pico cells and more than four-fold improvement in user throughput in the cluster. This has resulted from a reduction in the downlink block error rate (DL BLER) and an improvement in the spectral efficiency due to the informed triggering of the multiple radio streams as part of DL CoMP.

Index Terms—MIMO, DL CoMP, LTE, LTE-A, mmWave, machine learning, SVM, heterogeneous networks, SON, IoT, energy-efficient transmission.

I. INTRODUCTION

A. Background

THE *Downlink Coordinated Multi-Point* (DL CoMP) operation was first introduced in 3gpp Rel 11 for LTE-Advanced networks as a feature that improves data rates coverages and cellular capacity particularly at cell edge [1]. Combined with heterogeneous networks, DL CoMP is likely to continue play an important role in 5G networks, along with massive MIMO [2].

As far as the cellular *user equipment* (UE) is concerned, DL CoMP has several formats:

- **Joint Processing:** where data for a UE is available at more than one point participating in the data transmission in a time-frequency resource. These points (or base stations) are called the *CoMP cooperating set*. Alternatively, joint processing is also called *joint transmission*.
- **Dynamic Cell Selection:** where the UE serving cell can be changed on a per-subframe basis.
- **Coordinated Scheduling/Beamforming:** where one point in the CoMP cooperating set transmits data on the downlink, but coordinates with other points for user scheduling and beamforming decisions.

F. B. Mismar is a graduate student in the Department of Electrical and Computer Engineering, The University of Texas at Austin, Austin, TX, 78721, USA e-mail: faris.mismar@utexas.edu.

B. L. Evans is with The University of Texas at Austin email: bevans@ece.utexas.edu.

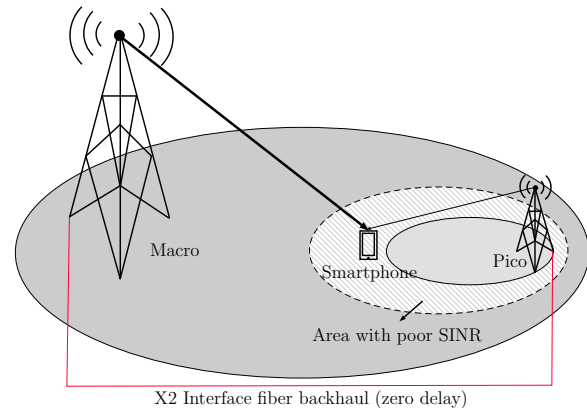


Fig. 1: Typical DL CoMP Setup in a Heterogeneous Network

The management of the DL CoMP measurement set may be based on *radio resource management* (RRM) measurements and the standards do not mandate a particular measurement though they specify the measurement should be based on either the *cell-specific reference symbol* (CRS) measurements or the *channel state information* (CSI). The CoMP cooperating set is determined by the higher layers such as the *radio resource control* (RRC) or the *medium access control* (MAC) layer [1].

Two common scenarios exist as far as DL CoMP implementation is concerned: *inter-* and *intra-*site. In a heterogeneous network setup, the focus is mostly on the inter-site implementation, where a point-to-point fiber with zero delay and large capacity backhaul connects the two base stations of two different transmit powers, as in Fig. 1.

B. Motivation

The demand for data traffic over cellular networks continues to increase with emphasis on low latency and reliability [3]. Heterogeneous networks are one of the most important solutions to increase the network capacity, where low power base stations are deployed along with the existing high power macro base stations. With the aid of low latency links connecting the low and high power nodes, a distributed MIMO channel can be formed to further bring data throughputs closer to the theoretical limits. This can be done via DL CoMP.

This paper motivates a dynamic, distributed, and optimum “network” MIMO channel composed of all the transmitting nodes in the DL CoMP cooperating set with the focus on the *joint processing* category of DL CoMP and with the use of

a machine learning algorithm residing in the base station to improve end-user experience while releasing the burden off the RF engineer to find an SINR threshold for DL CoMP to be triggered and save the environment by transmitting less power whenever possible.

In LTE-A, the cellular UE in *closed-loop spatial multiplexing* MIMO (CLSM) measures the channel and gives quantized feedback about the CSI in the form of either periodic or aperiodic reports, which typically contain *rank indicator*, *channel quality indicator*, and *precoding matrix information* (RI, CQI, PMI) [4], [5]. Since this CSI is measured by the receiver for the *transmit* channel, literature refers to it as CSIT [6]. Clearly, this is imperfect channel state information and no transmitting end has perfect knowledge of the channel. Thus, the cellular UE attempts to estimate a suitable CSI in order to maximize the throughput. This behavior is yet more important in the joint processing DL CoMP when done to multiple users as opposed to a single-user joint processing, where multi-user joint processing is more sensitive to CSI imperfections than single users, as found in [7].

In the standards body, 3gpp TS 36.213 specifies that the periodic wideband reporting of CQI is sent during subframes that satisfy the following expression [4]:

$$(10 \times n_f - N_{\text{OFFSET CQI}}) \bmod N_{pd} = 0$$

where n_f is the LTE system frame number (0–1023), k is the subframe number within the radio frame (0–9), N_{pd} is the CQI-PMI reporting period which has a minimum setting of 2 (i.e., report CQI every other subframe), and $N_{\text{OFFSET CQI}}$ is the reporting offset as defined in [4].

The CSIT is facilitated by the insertion of reference symbols (i.e., pilots) periodically inserted in the LTE resource grid. The subset of nodes in the cooperating set in which the CSIT is measured by the cellular UE and reported back is called the *CoMP measurement set*. DL CoMP algorithm uses this information to improve the downlink link adaptation and improve the performance on the downlink through joint transmission. We will measure the downlink performance in terms of the empirical CDF of the *signal to interference and noise ratio* (SINR), the average *block error rate* (BLER) on the *physical downlink shared channel* PDSCH channels, the average spectral efficiency per user, and the average end-user throughput on the downlink. We show that RF coverage measurements—namely the *reference signal received power* (RSRP)—were not impacted as a result of our contribution.

In this paper, we start from a requirement that the base stations receiving the CSIT reports from one cellular UE also receive CSIT information from all cell-edge connected cellular UEs (these are not many) prior to the DL CoMP algorithm to be triggered for a duration not exceeding 3 subframes (3 ms), which we call the collection period duration (T_{CoMP}). It is clear that this cellular UE and all other connected UEs have their serving radio link with the low power node and DL CoMP algorithm will assess

whether another radio link from the macro base station can be engaged. The choice of 3 subframes is to ensure a minimized time varying communication channel and ensure that cellular UEs have consistent space-time behavior. This requirement elicits a modification to the 3gpp standards body where N_{pd} is allowed to become unity.

C. Relevant Prior Work

In [8], the authors introduce a traffic analysis model for traffic analysis based on Markov chains and approximately compute the power in multi-cell environments in a joint transmission DL CoMP scheme. They introduce call admission control to improve the resource utilization based on transmission from multiple cells—an environment that resembles our setup. They also compute the effective throughput and probability of call blocking. We focus mostly on user perceived throughput and spectral efficiency without regards to the call blocking.

In [9], the authors applied a noncoherent joint transmission DL CoMP scheme to heterogeneous cellular networks, and used Rayleigh fading.

The performance of the zero forcing beamforming has been evaluated in [10] and the authors did so by randomly dropping the base stations in a two-dimensional plane for multiple times. There was no reference, however, to any particular morphology and a generic path loss model was used. Also, the work falls under CoMP coordinated scheduling/beamforming format.

Interference mitigation and handover management in CoMP-formed clusters is discussed in [11], [12]. The authors focused on joint transmission and showed outputs comparing performance with an approach similar to the approach taken in this paper; however, their clustering algorithm “affinity propagation based clustering” is intended to reduce backhaul utilization without harming end-user throughputs. In the algorithm discussed in this paper, the aim is to improve end-user throughput. Furthermore, we do not require the formation of star clusters as heterogeneous networks in CoMP are likely to serve a user capable of two receive streams in pairs composed of one high power macro and one low power node.

The authors in [13] use the dynamic cell selection scheme of DL CoMP. They, similar to [8], proposed a queuing model. They developed a cross-layer analytical model taking into consideration the time-varying channels. We on the other hand add a constraint to ensure minimized time varying communication channel. As they chose the dynamic cell selection scheme, they needed to deal with a “sleeping cell” concept, which is basically a cell that has received data for transmission to the UE where another cell in a given subframe actually transmitted the data to a given UE. We, on the other hand, focus on the joint transmission scheme where the UE is likely to receive data from multiple streams.

D. Contribution

The paper makes the following specific contributions:

- Use machine learning to derive the optimal conditions at which DL CoMP can be triggered “on the fly” instead of relying on the static DL CoMP configuration parameters from the radio engineer at the base station. See Section IV.
- Improve user downlink bitrate at the cell edge. See Section VI.
- Demonstrate that selection of the DL SINR triggering threshold at which DL CoMP is triggered as part of the RF optimization work done by RF engineers will cause sub-par downlink bitrates. See Section VI.
- Attempt to solve the capacity optimization problem from the base station instead of allowing the UEs to guess. See Section IV.

E. System Description

The system described in this paper is made of two modules:

- An inter-site DL CoMP operation in a heterogeneous network composed of a three-sectored macro base station and one pico base station per macro sector connected with negligible delay optical fiber effectively forming a *Cloud RAN* (or C-RAN for short) in an urban setting where most of the traffic is generated indoors. This operation is simulated using MATLAB.
- A machine learning algorithm using a *support vector machine* (SVM) classifier to derive optimum DL SINR triggering point for DL CoMP to operate if applicable. This algorithm is implemented in MATLAB.

F. Paper Organization and Notation

Section II describes the setup of the model. Section III lists the key assumptions made in running the simulations. In Section IV, we approach the problem from two angles: radio environment and machine learning. We detail the novel algorithm to trigger DL CoMP in Section V. Section VI shows the simulation results and justification of the results. We conclude the paper with Section VII and a summary of the findings and proposed ways forward.

Notation: Boldface lower and upper case symbols represent vectors and matrices respectively, and that includes both Latin and Greek alphabets. The column vector is grouped using (\cdot) . We use $\mathcal{N}_{\mathbb{C}}(\boldsymbol{\mu}, \boldsymbol{\Sigma})$ to denote the circular symmetric complex Gaussian distribution with mean $\boldsymbol{\mu}$ and covariance matrix $\boldsymbol{\Sigma}$. $\mathbb{E}[\cdot]$ denotes the expectation operator. The transpose operator is given by $(\cdot)^{\top}$ and the conjugate-transpose (i.e., Hermitian) operator is given by $(\cdot)^{\text{H}}$. We use the brackets $[\cdot]$ both normal or superscripted to denote discrete time. The Euclidian norm of a vector \mathbf{x} is given by $\|\mathbf{x}\|$. The inner product of two vectors is given by $\langle \cdot, \cdot \rangle$ and the \triangleq symbol means equal by definition. Indices on matrices and vectors are consistent with MATLAB notation with an M -by- N matrix with complex elements written as $\mathbb{C}^{M \times N}$ and the real and complex coordinate vector space of n dimensions are written as \mathbb{R}^n and \mathbb{C}^n respectively.

Finally, the indicator function $\mathbb{1}_{(\cdot)}$ is one if the condition in the parentheses is true and zero if false.

II. SETUP

Our setup for the macro base station entails a hexagonal cellular geometry of three cells, one pico cell per macro cell, non-stationary user equipment with two antennas that are randomly placed in the cell effectively forming a densification heterogeneous network setup, *frequency-division duplex* (FDD) operation, and fast fading and log-normal shadow fading. Pico base station is a *low power node* (LPN) and therefore we use pico and LPN interchangeably in the paper.

A. OFDM

We have used *orthogonal frequency division multiplexing* (OFDM). We use a subcarrier spacing, $\Delta f = 15$ kHz and a normal cyclic prefix of 7 OFDM symbols per slot or 14 OFDM symbols in 1 ms *transmit time interval* (TTI) with the transmit function being with respect to the base station (i.e., DL). The nature of OFDM orthogonality makes *zero-forcing* (ZF) estimation quite favorable in the analysis of this paper since OFDM modulation turns a frequency-selective MIMO channel into a set of parallel frequency-flat and single-tap MIMO channels.

B. Base Stations

The cells are hexagonal. Within each cell, cellular UEs are placed randomly, uniformly distributed over the cell. At the center of the cell is a macro base station with directional antennas. Small cells are placed so they coincide in the antenna null though in practice they should be placed in coverage holes, defined by suboptimal reference signal received power and SINR distribution.

For a base station to handle events such as when to trigger CoMP for a given cellular UE, a *configuration management* (CM) database is uploaded by the operator which allows coordinated cells to select candidates for CoMP on the basis of their estimated cell-specific reference symbol SINR, estimated as a function of their reported CQI values. In fact, the 3gpp standards do not specify which parameters or physical channel measurements trigger DL CoMP [1]. Operator settings are static in nature and can cause sub-optimal performance and end-user downlink throughput or excessive transmit power.

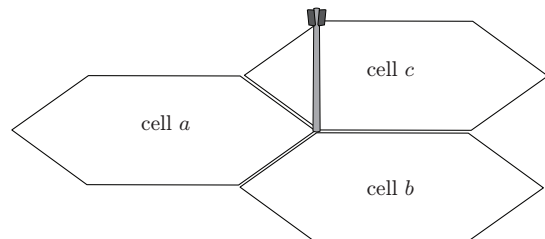


Fig. 2: Macro base station showing hexagonal geometry

For the purposes of simulation, cell edge is defined by traffic in the lower 5% of the distribution [14].

C. Propagation

No interference mitigation techniques have been implemented besides ZF to cancel intra-cell interference. We also treat inter-cell interference as noise. The average terrain height is assumed to be zero with the macro antenna height extending 25m above the terrain and the low power node mounted at 10m above the terrain.

All channels are independent of the transmitted signal (e.g., no channel-dependent power control) for the sake of simplicity of computations and in alignment with the 3gpp standards on the downlink [4].

We also used a variant of the semi-empirical COST 231 path loss model to predict the path loss and find the RF coverage levels at the cellular UEs.

D. User Equipment

Each cellular UEs i is assumed to be a 3gpp Rel-11 compliant smartphone. Based on whether admission control is set or hard-blocking occurs, i cannot exceed Q , which is the maximum number of UEs per cell. We will use LTE category-four devices. A category-four UE can handle up to two layers of spatial multiplexing and that includes DL CoMP [15]. These UEs are moving at an average speed of 5 km/h and are assumed to use zero forcing equalization.

III. KEY ASSUMPTIONS

Below we list the key assumptions for this algorithm. These assumptions still keep system model realistic. We also claim this is the worst case scenario of capacity demand in a dense urban environment.

- The computed DL SINR target threshold will be invalidated after T_{CoMP} TTIs.
- Due to technical limitations in the used simulator, DL CoMP is enabled for the entire DL CoMP coordinating set at once. Either all UEs in this TTI get DL CoMP enabled or none. The decision is done on the basis of a vote with a fixed threshold of 20%. While this assumption may seem relaxed, it is likely to happen since the UEs served by a low power node at the edge of coverage are likely to experience similar RF conditions due to proximity. This is true for both baseline and improved algorithms alike.
- The channel is a 2×2 distributed MIMO channel. This implies that only up to one macro base station and one low power node are engaged with one UE at any given time for a DL CoMP transmission. Cell edges spatial multiplexing gains may disappear where signal levels are low relative to interference as stated in [16], hence the importance of DL CoMP.
- All channels are independent of the transmitted signal (e.g., no channel-dependent power control) in alignment with 3gpp standards [4].

- Link adaptation, or *adaptive modulation and coding* (AMC), is completely under control by the simulator to allow reproducibility [14].
- While COST 231-Walfisch-Ikegami model extends to small cells in urban environments, COST 231-Hata was the algorithm chosen since the simulator has it built-in [14].
- The simulator has a choice for femto cells and no choice for pico [14]. We have used the femto base station and configured it to function as a pico in terms of the transmit power and noise figure. Both types have an omnidirectional antenna.

IV. PROBLEM

We break down the problem into two components: radio environment and machine learning.

A. Radio Environment

The list of the proposed radio environment parameters are listed in Table I. We have used the antenna pattern shown

TABLE I: Radio environment parameters

Parameter	Value
Bandwidth	10 MHz
Downlink center frequency	2100 MHz (Band 1)
Channel model type [†]	EPA5
LTE cyclic prefix	normal
Scheduling algorithm	Proportional Fair
Equalizer	Zero Forcing
Propagation model	COST231
Propagation environment	urban
Number of UEs per cell	10
UE device category	LTE CAT-4
LPN (i.e., pico base station) power	37 dBm
LPN antenna height	10 m
LPN antenna model	omnidirectional
Macro site geometry	hexagonal
Macro base station power	46 dBm
Macro base station antenna height	25 m
Macro base station antenna electrical tilt	4°
Macro base station antenna mechanical tilt	0°
Minimum coupling loss (36.104)	70 dB
Macro base station antenna model	Kathrein 742212 (X-pol)
Inter-site distance	100 m
Shadow fading margin standard deviation	8 dB
Shadow fading margin mean	0 dB
UE antenna gain	-1 dBi
BS noise figure	4 dB
UE noise figure	7 dB
UE height	1.5 m
UE average movement speed	5 km/h
Noise power density	-174 dBm/Hz

[†] i.e., the power delay profile.

in Fig. 3 in the simulation for the macro base station. The pico base stations use an omnidirectional antenna with a 0-dB gain.

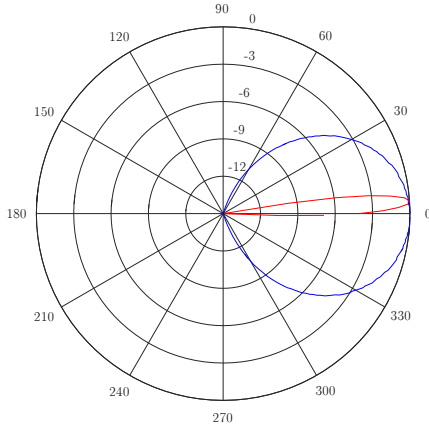


Fig. 3: 3D Antenna pattern used in simulation for the macro base station with 4° electrical tilt: elevation pattern (red) and azimuthal pattern (blue) [14]

For the i -th cellular UE at the k -th transmit interval, the received signal model with frequency flat narrowband assumptions is given by [17]:

$$\begin{aligned}
 \mathbf{r}_i[k] &= \underbrace{\sqrt{\frac{GE_s}{N_T}} \mathbf{H}_i \mathbf{F}_i \mathbf{s}_i[k]}_{\text{own signal}} \\
 &+ \underbrace{\mathbf{H}_i \sum_{\substack{j=0 \\ j \neq i}}^Q \sqrt{\frac{G_j E_{s,j}}{N_{T,j}}} \mathbf{F}_j \mathbf{s}_j[k]}_{\text{intra-cellular interference}} \\
 &+ \underbrace{\mathbf{v}[k]}_{\text{noise}}, \\
 k &= 0, \dots, T_{\text{CoMP}}; \\
 i &= 1, \dots, Q
 \end{aligned} \tag{1}$$

where $\mathbf{H}_i \in \mathbb{C}^{N_R \times N_T}$ is the normalized multivariate impulse response of a discrete-time system for user i , with N_R is the number of receive antennas and N_T is the number of transmit antennas. $\mathbf{F}_i \in \mathbb{C}^{N_T \times N_s}$ is the precoder matrix obtained through *block diagonalization* (BD) with $N_s \leq \min(N_R, N_T)$ being the number of spatially multiplexed data streams. The transmitted signal is $\mathbf{s}_i[k]$. The additive noise is $\mathbf{v}[k]$ which is $\sim \mathcal{N}_{\mathbb{C}}(\mathbf{0}, \sigma_v^2 \mathbf{I}_{N_R})$. σ_v^2 is the noise power density at the receiver. G is the large-scale channel gain for the current user i , E_s is the transmit energy per symbol. Finally, all quantities with a second index j are for the user j . The value of N_s could be either 1 or 2 depending on the CSIT feedback. The goal of BD precoding is to perfectly eliminate interference at each user due to others [17].

Clearly this enables us to write the estimated transmitted signal after ZF equalization:

$$\hat{\mathbf{s}}_i[k] = \mathbf{W}_{\text{ZF},i}^H \mathbf{r}_i[k] \tag{2}$$

with $\mathbf{W}_{\text{ZF},i} \in \mathbb{C}^{N_R \times N_T}$ being the ZF equalization matrix. Applying BD to DL CoMP, we obtain the joint transmission format.

Further, define *per-user achievable data rate with quantized CSIT* for i -th cellular UE as [17]:

$$C_i \triangleq \mathbb{E} \left[\log_2 \det \left(\mathbf{I}_{N_R} + \frac{\text{SINR}_i}{N_{T,i}} \mathbf{H}_i \mathbf{F}_i \mathbf{F}_i^H \mathbf{H}_i^H \right) \right] \tag{3}$$

where the expectation is taken with respect to the channel and its corresponding precoder realization.

Let us define SNR_i in linear scale (i.e., non-dB) as a direct estimate from the CQI reported by the cellular UE i . For simulation purposes define $\text{SNR}_i^{[k]}$ reported by the receiver to the CoMP measurement set at TTI k as:

$$\text{SNR}_i^{[k]} \triangleq \frac{GP_s}{N_0 B} \frac{|\mathbf{H}_i \mathbf{F}_i|^2}{N_T} \tag{4}$$

where N_0 is the noise power density measured at the cellular UE receiver and B is the bandwidth of the transmission. P_s is the transmit power.

We shall treat cell-edge interference as Gaussian noise with the argument that we have many interferers at the cell edge thus changing $\mathbf{v}[k]$ in Equation 1 into $\mathbf{z}[k]$ which is now noise plus inter-cellular interference with the Gaussianity justified on the basis of the Central Limit Theorem thereby making $\mathbf{z} \sim \mathcal{N}_{\mathbb{C}}(\mathbf{0}, \mathbf{P}_{\mathbf{z}})$.

With a group of interfering radio links N at the cell edge with an interfering received power of P_i , one can write the received $\text{SINR}_i^{[k]}$ as:

$$\begin{aligned}
 \text{SINR}_i^{[k]} &\triangleq \frac{GP_s}{N_0 B + \sum_{\substack{j=0 \\ j \neq i}}^N P_{z,j}} \frac{|\mathbf{H}_i \mathbf{F}_i|^2}{N_T} \\
 &= \frac{GP_s}{N_0 B + \sum_{\substack{j=0 \\ j \neq i}}^N G_j P_{s,j}} \frac{|\mathbf{H}_i \mathbf{F}_i|^2}{N_T}
 \end{aligned} \tag{5}$$

where $P_{z,j}$ is the cell-edge interference due to cell j .

Standards do not require that the UE reports its SINR [18], [19], and therefore a one-to-one relationship between $\text{SINR}_i^{[k]}$ and CQI has been proposed for convenience [14], [20] treating the cell-edge interference as additive noise as mentioned earlier. This means that SINR is now basically SNR. Fig. 4 shows the mapping we have used with this in mind. If UE were to report its SINR, which is typically a floating-point number, then a quantized feedback of 32 bits is required (for IEEE 754-2008 single precision floating-point format) as opposed to CQI which requires only 4 bits. This minimizes the signaling overhead in favor of the user plane capacity.

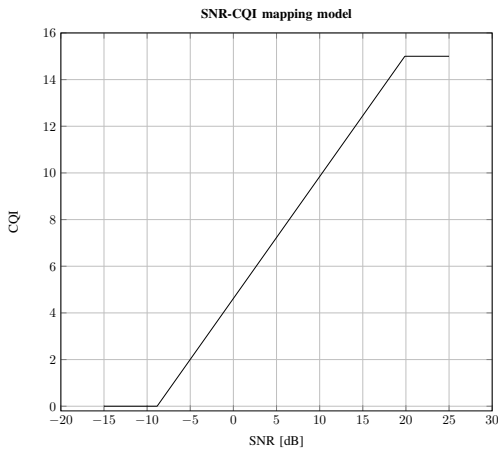


Fig. 4: Relationship between SNR and CQI in LTE [14], [20]

Whether BLER is within acceptable H-ARQ target value or not defines the supervisory signal labels of the machine learning algorithm, as discussed in Section IV-B. BLER is measured with respect to several inputs such as SINR and *modulation and coding scheme* (MCS). BLER-free transmission is generally not achieved due to channel imperfections and finite block length of codewords [17].

B. Machine Learning

The SVM classifier [21] is a supervised machine learning model that we have used in the implementation of this algorithm.

We define the learning features in a matrix $\mathbf{X} \triangleq (\mathbf{x}_1, \mathbf{x}_2)$ as in Table II, collected from all the cellular UEs in the CoMP coordinated set during the time frame of T_{CoMP} .

TABLE II: Proposed machine learning features

Feature	Description
\mathbf{x}_1	CQI reports
\mathbf{x}_2	RSRP measurement reports

The reason why we have chosen CQI and RSRP is because they are two physical channel measurement quantities that are not directly correlated. RSRP is measured over the reference symbols (15 kHz of width) while CQI is an indication of the wideband SINR. If the quantities were correlated or close to correlated, we would have a phenomenon known as *collinearity* which basically means that one feature can be linearly predicted from the other with a substantial degree of accuracy. This in turns may not give valid results about our predicted target.

Standards specify target of 0.1 block error probability for a valid modulation scheme and *transport block size* (TBS) [4]. This value is called the *hybrid automated repeat request* (H-ARQ) target. BLER is calculated every codeword or transport block. This effectively throws an optimization problem at the UE to estimate a suitable CSI in order to

maximize the mutual information (or loosely, the throughput C) as follows [22]:

$$\begin{aligned}
 C_i = \text{maximize:} & \quad \mathcal{I}(X; Y | \text{CSI}) \\
 & \quad \pi = p(X) \\
 \text{subject to:} & \quad \text{BLER} \leq 0.1, \\
 & \quad P_X \leq P_{\text{max}}
 \end{aligned}$$

where X is the transport block transmitted to the UE i at time k from the base station with power P_X and Y is the received transport block. π is the probability distribution of X . $\mathcal{I}(X; Y | Z)$ is the conditional mutual information between X and Y conditioned on Z . This optimization problem has no closed-form solution albeit convex since the mutual information is basically concave. Attempting to solve this with the aid of samples from all cellular UEs in a base station or over a CoMP coordinating set and machine learning is the essence of what this paper is solving.

BLER values fulfilling the H-ARQ target basically define the supervisory signal labels of the supervised machine learning algorithm, where $y_i[k] \leftarrow 1$ for a fulfillment of the target for the UE i and $y_i[k] \leftarrow 0$ if the BLER exceeded the H-ARQ target for the same UE. A dataset is called *imbalanced* if the number of positive classes $y_i[k] \leftarrow 1$ is far more than $y_i[k] \leftarrow 0$. Since this is a problem we face, no split of the datasets to training and test data is performed.

With features \mathbf{X} and supervisory signal labels \mathbf{y} being gathered at the CoMP cooperating set base stations, all what is left is for these base stations is to derive the decision whether the DL CoMP algorithm will kick-in for this cellular UE on the basis of the machine learning algorithm described.

We have used Bayesian optimization and K -fold cross-validation with $K = 5$ in order to tune the hyperparameters as shown in Table III. Optimality is measured with respect to the minimum loss objective function [23].

TABLE III: SVM classifier hyperparameters

Hyperparameter	Search range
γ	[0, 1]
C	[0, 1]
Kernel	{gaussian, linear, polynomial*}
Normalization	true, false

* Orders 2, 3, and 4.

V. ALGORITHM

The novel algorithm to trigger DL CoMP in the coordinating set is shown in Algorithm 1.

VI. SIMULATION RESULTS

With an aim to have reproducibility in this paper, we have used the Vienna LTE-A Downlink System Level Simulator [14] running on MATLAB. MATLAB requires that The Mapping Toolbox™ and Statistics and Machine Learning Toolbox™ be installed to use machine learning required to implement Algorithm 1.

Algorithm 1 Improved DL CoMP in Heterogeneous Networks

Input: Improved DL CoMP feature ON, ε misclassification error threshold, feature collection period T_{CoMP} , current triggering DL SINR, Q UEs reported CQI and RSRP.

Output: Triggering decision for DL CoMP for all Q UEs in $T_{\text{CoMP}} - 1$ TTIs

```

1: repeat
2:   for  $k \leftarrow 1$  to  $T_{\text{CoMP}}$  do
3:     for  $j \leftarrow 1$  to  $Q$  do
4:       Store measurements reported by all UEs  $j$  during all times  $k$ :
5:          $[\tilde{x}_1]_{(j,k)} \leftarrow \text{CQI}$ 
6:          $[\tilde{x}_2]_{(j,k)} \leftarrow \text{RSRP}$ 
7:          $[\tilde{x}_3]_{(j,k)} \leftarrow \text{DL BLER}$  {use BLER to derive supervisory label}
8:         if  $([\tilde{x}_3]_{(j,k)} \leq 0.1)$  then
9:            $[\tilde{y}]_{(j,k)} \leftarrow 1$ 
10:        else
11:           $[\tilde{y}]_{(j,k)} \leftarrow 0$ 
12:        end if
13:      end for
14:    end for
15:  Vectorize learning features and supervisory labels:
16:   $\mathbf{x}_1 \leftarrow \text{vec}(\tilde{\mathbf{x}}_1)$ 
17:   $\mathbf{x}_2 \leftarrow \text{vec}(\tilde{\mathbf{x}}_2)$ 
18:   $\mathbf{y} \leftarrow \text{vec}(\tilde{\mathbf{y}})$ 
19:  Drop all rows with  $\pm\infty$  values. {drop missing values}
20:   $\mathbf{X} \leftarrow [\mathbf{x}_1, \mathbf{x}_2]$  {dataset is now  $[\mathbf{X}_{\text{training}} | \mathbf{y}_{\text{training}}]$ }
21:
22:  Perform a search with three-fold cross-validation grid search on  $[\mathbf{X}_{\text{training}} | \mathbf{y}_{\text{training}}]$  to find the optimum hyperparameters of the SVM classifier over the search ranges defined in Table III.
23:  Train SVM classifier with  $\mathbf{X}_{\text{training}}, \mathbf{y}_{\text{training}}$  using the optimal parameters found above to find  $\hat{\mathbf{y}}$ .
24:
25:  Compute  $\text{Err} = \frac{1}{N} \sum_i \mathbb{1}_{y_i \neq \hat{y}_{i}}$ 
26:  if  $(\text{Err} > \varepsilon)$  then {SVM performance is unacceptable, do not override operator-entered settings.}
27:    DL  $\text{SINR}_{\text{target}}^{[T+1]} \leftarrow$  operator-entered DL  $\text{SINR}_{\text{target}}$ 
28:  else{SVM performed well, override operator-entered settings.}
29:    DL  $\text{SINR}_{\text{target}}^{[T+1]} \leftarrow -\infty$  {Enable DL CoMP in this TTI}
30:  end if
31:
32:  Use DL  $\text{SINR}_{\text{target}}^{[T+1]}$  for  $T_{\text{CoMP}} - 1$  more TTIs
33: until simulation time ends
34: return
    
```

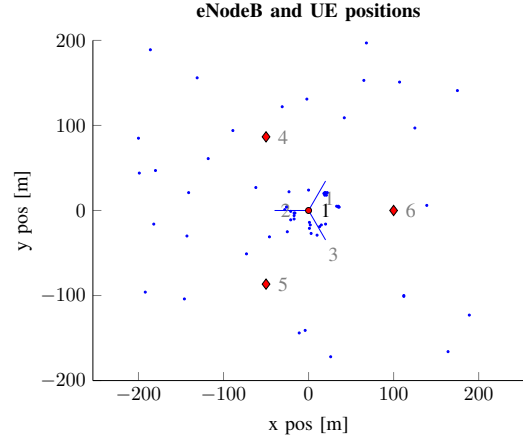


Fig. 5: Simulated LTE network showing base stations in red and UEs in blue

The simulated network is comprised of a three-sector macro, 3 pico base stations, and UEs as shown in Fig. 5.

The simulation parameters are summarized in Table IV.

TABLE IV: Simulation parameters

Parameter	Value
Number of UEs Q per cell	10
Number of cells per cluster	6
Number of cell tiers	1
T_{CoMP}	3 TTIs
Simulation time	60 TTIs
ε	12%

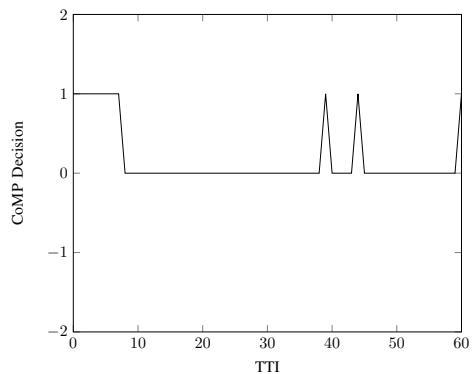
In Fig. 6, it is clear that the baseline static algorithm made decisions to enable or disable CoMP in the coordinated set for users where the improved dynamic algorithm made an opposite decision. We assert that the reason for this is simply because the dynamic algorithm predicted that DL BLER would meet the H-ARQ target better than what the UEs would have guessed when they reported their CQI values.

Tables V, VI, and VII outline the *key performance indicators* (KPIs) and show that the proposed CoMP algorithm shows a higher cell edge UE throughput and lower average block error rate with same power and almost equal average wideband SINR as proxied by the average reported CQI. Improved figures are in **boldface**.

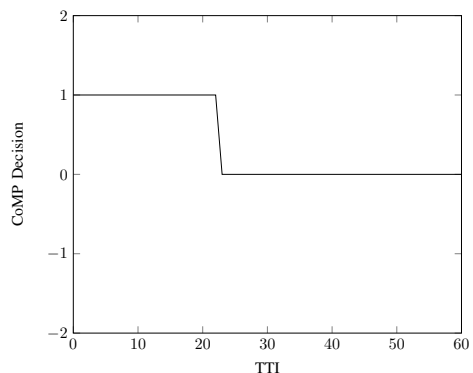
TABLE V: KPIs for both Baseline and Dynamic DL CoMP schemes

Cluster	UE Throughput [Mbps]					
	Baseline [†]			Dynamic		
	Peak	Average	Edge	Peak	Average	Edge
Macro	1.85	0.78	0.00	1.47	0.71	0.10
Pico	4.02	1.94	0.66	3.25	1.89	0.88
Overall	3.90	1.36	0.02	2.70	1.30	0.11

[†] Baseline DL CoMP enabling is the static DL CoMP algorithm with a trigger of DL SINR_{min} of 3 dB.



(a) Baseline DL CoMP algorithm (static DL CoMP algorithm)



(b) Proposed DL CoMP algorithm (dynamic DL CoMP algorithm)

Fig. 6: DL CoMP being enabled (state = 1) and disabled (state = 0) for both baseline (left) and the proposed algorithm (right) over the same TTIs

TABLE VI: Link-level metrics comparison between DL CoMP schemes

Scenario	Average		
	DL BLER	CQI	RSRP [dBm]
Baseline [†]	15.05%	5	-65.98
Dynamic CoMP	14.96%	5	-65.98

[†] Baseline DL CoMP enabling is the static DL CoMP algorithm with a trigger of DL SINR_{min} of 3 dB.

TABLE VII: Spectral efficiency comparison between DL CoMP schemes

Scenario	Average Spectral Efficiency [bits/symbol]	
	LPN only	Cluster
Baseline [†]	2.41	1.75
Dynamic CoMP	2.50	1.80

[†] Baseline DL CoMP enabling is the static DL CoMP algorithm with a trigger of DL SINR_{min} of 3 dB.

VII. CONCLUSIONS

As we were able to improve the spectral efficiency on the downlink and achieve higher cell edge data rates, the average transmit power requirement can be further reduced to meet the target SINR required to achieve the data rate; therefore reducing the base station power requirement and the CO₂ emissions. This constitutes the essence of *Green Cellular Networks*, an area that can benefit immensely from dynamically finding optimum power levels while saving the environment.

We have only used two learning features for SVM. A potential way forward is to try the same algorithm with feedforward deep neural networks or an ensemble classifier such as XGBoost instead of SVM and consider adding more learning features. An example feature is the SINR measurement per UE connected to a co-sited cell on a different frequency such as mmWave or sub-6 GHz carriers. Furthermore, user location alongside with RSRP—user location can be obtained from GPS reports if 3gpp allows them to be reported or estimated via positioning reference signals in LTE/LTE-A—is one way to add more learning features to the algorithm.

With operators desiring to cut operational expenditure, further radio access features can be implemented with machine learning, effectively minimizing the need of continuous tuning of parameters. Handover thresholds and power control can be two good candidates for similar research in the near future to further improve *self-optimizing networks* (SON) capabilities where relevant suggestions were made [24]. With the wide-spread adoption of *Internet of Things*, devices can also reveal their use capabilities (e.g., sensor, camera, smartphone, etc.) and that could be factored in for different thresholds for different device types. In fact, with the advent of mmWave and 5G communications where urban pico and femto cells will be operating along macro base stations in spectrum bands that have tens of gigahertz of bandwidth in smaller cell radii (50–200m) [25], the need to investigate CoMP to aid either both outdoor or indoor propagation may prove useful, especially that at mmWave carrier frequencies, the transceiver impairments hinder the spectral efficiency particularly at the high SNR regime [26]. Improved DL CoMP may be well exploited even in line of sight distributed MIMO cases with mmWave due to these impairments.

As we only considered the case of one macro cell to one pico cell densification heterogeneous network setup, one area worth looking into is a multi-tiered cluster (i.e., more than just one macro and three picos)—something that resembles an actual deployment of a network. This way the impact on cell-edge throughput besides reduced noise and fading effects is more realistic. In fact, attempting to restrain the relaxed assumption of all or none users receiving data per TTI proves very useful, especially that in cellular systems, more than one user per TTI are likely to be receiving data, but not all are likely to be in DL CoMP.

Besides the requirement of a very reliable and high speed low latency link between base stations, introducing machine learning to base stations require additional memory and CPU cycles. With floating point arithmetic being costly, it could be an interesting venue to compute the complexity and cost of such an introduction.

APPENDIX

A. Vienna Simulator Entry Point MATLAB Code

The entry point code only is available on GitHub [27]. The Vienna LTE-A Downlink Link-Level Simulator code

has to be downloaded separately [17]. The code starts execution from `Main_File.m`.

REFERENCES

- [1] 3GPP, “Coordinated Multi-Point Operation for LTE,” 3rd Generation Partnership Project (3GPP), TR 36.819, Sep. 2013. [Online]. Available: <http://www.3gpp.org/dynareport/36819.htm>
- [8] S. Y. Kim and C. H. Cho, “Call Blocking Probability and Effective Throughput for Call Admission Control of CoMP Joint Transmission,” *IEEE Transactions on Vehicular Technology*, vol. 66, no. 1, pp. 622–634, Jan 2017.
- [9] G. Nigam, P. Minerio, and M. Haenggi, “Coordinated Multipoint Joint Transmission in Heterogeneous Networks,” *IEEE Transactions on Communications*, vol. 62, pp. 4134–4146, 2014.
- [10] P. Xia, C. H. Liu, and J. G. Andrews, “Downlink coordinated multipoint with overhead modeling in heterogeneous cellular networks,” *IEEE Transactions on Wireless Communications*, vol. 12, no. 8, pp. 4025–4037, August 2013.
- [11] H. Zhang, C. Jiang, J. Cheng, and V. C. Leung, “Cooperative Interference Mitigation and Handover Management for Heterogeneous Cloud Small Cell Networks,” 2015. [Online]. Available: <http://arxiv.org/pdf/1504.08076.pdf>
- [12] S. Wesemann and G. Fettweis, “Decentralized Formation of Uplink CoMP Clusters Based on Affinity Propagation,” *International Symposium on Wireless Communication Systems (ISWCS)*, pp. 850–854, 2012.
- [13] A. Alorainy and M. J. Hossain, “Cross-Layer Performance of Downlink Dynamic Cell Selection with Random Packet Scheduling and Partial CQI Feedback in Wireless Networks with Cell Sleeping,” V. Jungnickel, K. Manolakis, W. Zirwas, B. Panzner, V. Braun, M. Lossow, M. Sternad, R. Apelfrojd, and T. Svensson, “The role of small cells, coordinated multipoint, and massive MIMO in 5G,” *IEEE Communications Magazine*, vol. 52, no. 5, pp. 44–51, May 2014.
- [3] “Ericsson Mobility Report,” November 2016. [Online]. Available: <https://www.ericsson.com/assets/local/mobility-report/documents/2016/ericsson-mobility-report-november-2016.pdf>
- [4] 3GPP, “Evolved Universal Terrestrial Radio Access (E-UTRA); Physical layer procedures,” 3rd Generation Partnership Project (3GPP), TS 36.213, Dec. 2008. [Online]. Available: <http://www.3gpp.org/dynareport/36213.htm>
- [5] J. Acharya, L. Gao, and S. Gaur, *Heterogeneous Networks in LTE-Advanced*, 1st ed. Wiley, 2014.
- [6] A. Goldsmith, *Wireless Communications*. New York, USA: Cambridge, 2009.
- [7] D. Jaramillo-Ramirez and M. Kountouris and E. Hardouin, “Coordinated Multi-Point Transmission With Imperfect CSI and Other-Cell Interference,” *IEEE Transactions on Wireless Communications*, vol. 14, no. 4, pp. 1882–1896, April 2015.
- IEEE Transactions on Wireless Communications*, vol. PP, no. 99, pp. 1–1, 2017.
- [14] M. Taranetz, T. Blazek, T. Kropfreiter, M. K. Müller, S. Schwarz, and M. Rupp, “Runtime Precoding: Enabling Multipoint Transmission in LTE-Advanced System Level Simulations,” *IEEE Access*, vol. 3, pp. 725–736, June 2015.
- [15] 3GPP, “Evolved Universal Terrestrial Radio Access (E-UTRA); User Equipment (UE) radio access capabilities,” 3rd Generation Partnership Project (3GPP), TS 36.306, 2015. [Online]. Available: <http://www.3gpp.org/dynareport/36306.htm>
- [16] T. L. Marzetta, “Noncooperative Cellular Wireless with Unlimited Numbers of Base Station Antennas,” *IEEE Transactions on Wireless Communications*, vol. 9, no. 11, pp. 3590–3600, November 2010.
- [17] M. Rupp, S. Schwarz, and M. Taranetz, *The Vienna LTE-Advanced Simulators: Up and Downlink, Link and System Level Simulation*, 1st ed., ser. Signals and Communication Technology. Springer Singapore, 2016.
- [18] 3GPP, “Evolved Universal Terrestrial Radio Access (E-UTRA); Physical layer measurements,” 3rd Generation Partnership Project (3GPP), TS 36.214, Dec. 2015. [Online]. Available: <http://www.3gpp.org/dynareport/36213.htm>
- [19] —, “Evolved Universal Terrestrial Radio Access (E-UTRA); Radio Resource Control (RRC); Protocol specification,” 3rd Generation Partnership Project (3GPP), TS 36.331, Sep. 2015. [Online]. Available: <http://www.3gpp.org/dynareport/36331.htm>
- [20] C. Mehlführer, M. Wrulich, J. C. Ikuno, D. Bosanska, and M. Rupp, “SIMULATING THE LONG TERM EVOLUTION PHYSICAL LAYER,” Glasgow, Scotland, Aug. 2009. [Online]. Available: https://publik.tuwien.ac.at/files/PubDat_175708.pdf
- [21] C. Cortes and V. Vapnik, “Support-Vector Networks,” in *Machine Learning*, 1995, pp. 273–297.
- [22] T. Cover and J. Thomas, *Elements of Information Theory*. John Wiley and Sons, 2006.
- [23] Mathworks Inc. Support Vector Machines. [Online]. Available: <https://www.mathworks.com/help/stats/fitcsvm.html>
- [24] I. da Silva, Y. Wang, F. B. Mismar, and W. Su, “Event-based performance monitoring for inter-system cell reselection: A SON enabler,” in *Wireless Communication Systems (ISWCS), 2012 International Symposium on*, Aug 2012, pp. 6–10.
- [25] Farooq Khan and Jerry Pi, “Millimeter-wave Mobile Broadband: Unleashing 3-300GHz Spectrum,” January 2011. [Online]. Available: <http://wncn2011.ieee-wncn.org/tut/t1.pdf>
- [26] T. S. Rappaport, R. W. Heath Jr., R. C. Daniels, and J. N. Murdock, *Millimeter Wave Wireless Communications*. New Jersey, USA: Prentice Hall, 2015.
- [27] F. B. Mismar. DL CoMP Machine Learning Code. [Online]. Available: <https://github.com/farismismar/DL-CoMP-Machine-Learning>